Acta Cryst. (1994). A**50**, 253–257

The Ultrasound-Induced Narrowing Effect of Rocking Curves in Strained Silicon Crystals

By E. Zolotoyabko, B. Sander and Y. Komem

Department of Materials Engineering, Technion-Israel Institute of Technology, Haifa 32000, *Israel*

and B. Kantor

Department of Electrical Engineering, Technion-Israel Institute of Technology, Haifa 32000, *Israel*

(*Received* 23 *April* 1993; *accepted* 12 *October* 1993)

Abstract

Surface acoustic waves were combined with double-crystal X-ray diffractometry in order to study strained silicon crystals. A narrowing effect in the rocking curves was observed owing to the ultrasound-induced modification of the X-ray trajectories. It is shown that the narrowing effect is strongly related to the lattice strain and can be used to increase the strain sensitivity of the X-ray diffraction technique.

1. Introduction

Dynamical X-ray diffraction under the influence of ultrasound (US) is a promising way to measure small lattice distortions in almost perfect crystals. High-frequency US with a wavelength λ_s satisfying the condition

$$\lambda_s < \tau, \tag{1}$$

where τ is the extinction length, effectively mixes the X-ray waves corresponding to different branches of the dispersion surface (separated by a gap, $\Delta k_o = 2\pi/\tau$, in reciprocal space). In the case of a perfect crystal, US-induced interaction between the X-ray waves leads to the creation of new gaps on the dispersion surface, Δk_n, and, consequently, to the formation of angular satellites in the diffraction spectrum, owing to coherent scattering on the acoustic superlattice (Kohler, Mohling & Peibst, 1974; Entin & Assur, 1981; Chapman, Colella & Bray, 1983). The angular width of the nth-order satellite is expressed as

$$\Delta\Theta_n = \Delta k_n/H = |J_n(Hw)|\Delta\Theta_o, \tag{2}$$

where $J_n(Hw)$ is the Bessel function of the nth order, H is the reciprocal-lattice vector, w is the US amplitude and $\Delta\Theta_o = \Delta k_o/H$ is the width of the base diffraction maximum. Thus, the angular widths of the satellites and their contribution to the diffraction intensity can be controlled by varying the US amplitude. For example, in the limit of weak US ($Hw < 1$), the angular width of the first-order satellite (one-phonon scattering process) is

$$\Delta\Theta_1 = |J_1(Hw)|\Delta\Theta_o \simeq Hw\Delta\Theta_o. \tag{3}$$

Consequently, the satellite contribution to the diffraction intensity $\Delta I \sim \Delta\Theta_1$ increases proportionally with w (Entin & Assur, 1981). This effect was used to measure a weak acoustic field ($Hw << 1$) in acousto-optical devices integrated on a silicon substrate (Zolotoyabko, Jacobsohn, Shechtman, Kantor & Salzman, 1992).

The appearance of narrow satellites [since, according to (3), $\Delta\Theta_1 < \Delta\Theta_o$ when $Hw < 1$] makes the diffraction process very sensitive to the strain, δ, in a crystal (Zolotoyabko, 1992). The presence of strain under appropriate conditions can even lead to the suppression of the satellite formation and, consequently, to qualitatively different behaviour of the diffraction intensity I under US excitation. In fact, a substantial decrease of I with increase of w (when $Hw < 1$) was observed in elastically strained crystals (Iolin, Raitman, Kuvaldin & Zolotoyabko, 1988; Zolotoyabko & Panov, 1992). This behaviour confirms the assumption that in distorted crystals the satellite formation is suppressed within the angular range of $\Delta\Theta \simeq \delta$, since in this range the diffraction intensity is already 'excited' by the strain gradient. Moreover, in the presence of strains, the US stimulates the transitions between the branches of the dispersion surface, leading to a modification of the X-ray trajectories inside the crystal and to the removal of part of the X-rays from the diffracted beam (Iolin, 1987). Some manifestations of such a mechanism in the integral diffraction intensity (new *Pendellösung* effect, which depends on the strain gradient and US frequency) were studied elsewhere (Zolotoyabko & Panov, 1992). However, the partial transfer of X-rays from a diffracted to the incident beam should lead to an additional narrowing of the diffraction profile under US excitation.

In this work, we present and discuss the narrowing effect of X-ray diffraction rocking curves in strained silicon crystals.

Acta Crystallographica Section A
ISSN 0108-7673 © 1994

2. Experimental

Double-crystal X-ray diffraction measurements were carried out in the Bragg scattering geometry with Cu $K\alpha$ radiation. An incident X-ray beam was formed by means of a Soller collimator in combination with a 0.2 mm slit in the scattering plane. A piece (12 × 20 mm) of a (001)Si wafer, covered on both surfaces with an amorphous Si_3N_4 protection layer (150 nm thick), was used as the first (reference) crystal. Square silicon samples (10 × 10 mm) were cut from a 6 in (001)Si wafer (650 μm thick) used as a substrate for very large scale integration (VLSI) of microelectronic devices. One edge of each sample was polished to provide a good contact with a piezoelectric transducer for acoustic-wave propagation. The transducer was made by using conventional photolithography and depositing interdigital aluminium electrodes, having a period $D = 12$ μm, on the surface of a rectangular $LiNbO_3$ single-crystalline plate (10 × 15 mm) with a thickness of 500 μm. The transducer generated Rayleigh surface acoustic waves with a base frequency of $\nu_o = 281.6$ MHz, as measured by the acoustic return loss response. The polished edge of the transducer was glued to the polished edge of the sample (as shown in Fig. 1) by heating a photoresist at 373 K for 1 h. The photoresist played, in fact, the role of an intermediate layer for the US waves propagating into the silicon sample. The sample–transducer assembly was mounted on a diffractometer and (004)Si rocking curves were measured at several points of the polished surface along an x axis parallel to the $[2\bar{2}0]$ direction of the sample (see Fig. 1). Measurements were carried out without US as well as under US excitation at a frequency ν_o [which satisfies condition (1)], with a piezotransducer voltage $U = 9.2$ V.

3. Results and discussion

Typical rocking curves measured in samples without US excitation along points marked as $x = 1, \ldots, 6$ in Fig. 1 are shown in Fig. 2. The distance between two neighbouring x points is approximately 1.5 mm. One can see that the rocking curve at point 1 has a Lorentzian-like shape with a full width at half-maximum (FWHM) $\Gamma_1 = 5.9$ s, which is a little larger than the theoretically predicted value of $\Gamma_{th} = 4.6$ s for a perfect silicon crystal. Curve 2 is already broader and the FWHM $\Gamma_2 = 6.8$ s. In curve 3, the broadening increases to FWHM $\Gamma_3 = 9.6$ s. In the next curve, 4, the FWHM $\Gamma_4 = 14.4$ s. In addition, curve 4 exhibits an asymmetry with a shoulder on the right side of the diffraction profile. This shoulder is clearly seen in curves 5 and 6, making their shape strongly nonsymmetric. The angular position of the shoulder in curve 6 is $\Delta\Theta_{sh} = 14.4''$, which corresponds to the maximum strain that prevails in the sample, having a value of $\delta_m = \Delta\Theta_{sh} \cot \Theta_B \simeq 10^{-4}$ (where Θ_B is the Bragg angle and $\Delta\Theta_{sh}$ is measured in rad). All the rocking curves that are shown in Fig. 2 have shape distortions resulting from an inhomogeneous strain field in the sample. The source of strain is not very important for further discussion, but it is assumed that the strain field was introduced by the glueing procedure. Owing to the difference between the Si and $LiNbO_3$ thicknesses, a small amount of the photoresist leaked to the lower silicon surface and led (after heating) to some sample bending around the y axis, parallel to the sample–transducer boundary (see Fig. 1). In this case, the strain increases with increasing distance from the boundary, along the x direction.

Under US excitation, all the rocking curves along the six measuring points exhibit a narrowing effect. Typical examples of this effect in the rocking curves

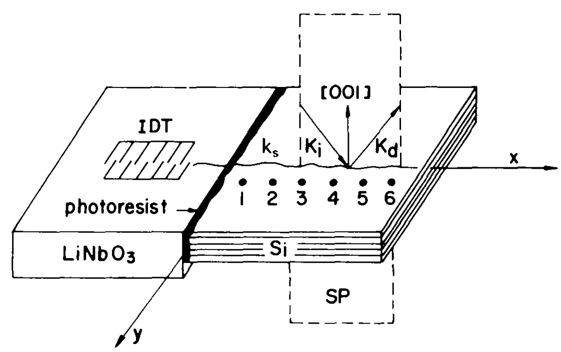

Fig. 1. Experimental layout of the sample–transducer assembly under X-ray beams. IDT is the aluminium interdigital transducer; x is the direction of sample scanning; 1, ..., 6 are the measurement points; k_s is the ultrasound wave vector; SP is the scattering plane, which is defined by the wave vectors of the incident and diffracted X-rays (K_i and K_d, respectively).

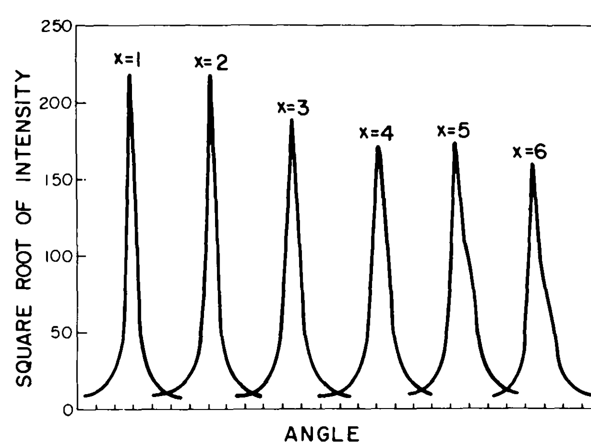

Fig. 2. (004)Si rocking curves (square root of intensity) obtained at points $x = 1, \ldots, 6$ (shown in Fig. 1) of a strained crystal. The curves are shifted from the origin for a better resolution of their shape. The 'Angle' axis is marked off in divisions of 18''.

at points $x = 2$ and $x = 5$ are shown in Figs. 3 and 4, respectively. We shall discuss the narrowing effect in terms of the dispersion surface (DS) and its modification by US.

The standard hyperbolic DS in the two-beam approximation is shown in Fig. 5. For a perfect crystal, the tie points on the DS are stable and the vertices of the hyperbola (points a and b in Fig. 5) contribute mostly to the diffraction intensity. In a strained crystal, there is a set of different DSs and at a given point the variation of the DS is determined by the strain gradient. However, as shown by Penning & Polder (1961), the set of DSs can be replaced by a single DS with movable tie points, reflecting the variation of the Bragg condition along the X-ray trajectory. Such modification of the DS greatly affects the diffraction process. Consider, for example, the incident X-ray wave near the entrance surface to be away from the exact Bragg condition. Such a wave excites states 1 and 6 on the DS (see Fig. 5). The excitations of states 1 and 6 do not contribute to the diffraction intensity in a perfect crystal because the group velocity (normal to the DS) is nearly parallel to the direction of the incident beam, *i.e.* oriented toward the 0 node of the reciprocal lattice. However, in a strained crystal, points 1 and 6 move under the strain gradient along the DS branches (Penning, 1966). The direction of movement is determined by the sign of the strain gradient and if, for example, the movement takes place from left to right (see Fig. 5), point 1 transforms into point 3, which already contributes to the diffraction because the group velocity here is almost parallel to the direction of the diffracted beam (towards the H node). The diffraction range is correspondingly expanded, resulting in broadening of the rocking curves (as was observed in the present experiment; see data without US in Fig. 2) and in the increase of integral diffraction intensity predicted by the classical theories of Penning & Polder (1961) and Kato (1963, 1964). It should be mentioned that in this case point 6 will never contribute to the diffraction intensity. The transformation of point 6 (instead of point 1) will be essential in the case of the strain gradient having the opposite sign (which leads to the movement of tie points from right to left).

The introduction of an US wave modifies drastically the movement of tie points along the DS. If the US wave vector $k_s = 2\pi/\lambda_s$ is larger than the gap $\Delta k_o = 2\pi/\tau$ [this condition is identical to (1)], the US-induced mixing of states 2 and 4, located on the different DS branches and separated by k_s, leads to the interbranch 2–4 jumping process. Thus, apart from the previous 1–2–3 trajectory (see Fig. 5), the second possible trajectory, 1–2–4–5, appears (Iolin, 1987). The finite state 5, according to the direction of group velocity, does not contribute to the diffraction intensity. In other words, the US rejects part of the

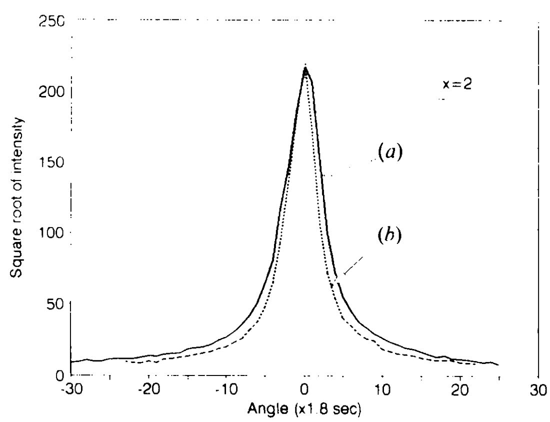

Fig. 3. (004)Si rocking curves (square root of intensity), measured at point $x = 2$ (shown in Fig. 1), (a) without and (b) with ultrasonic excitation.

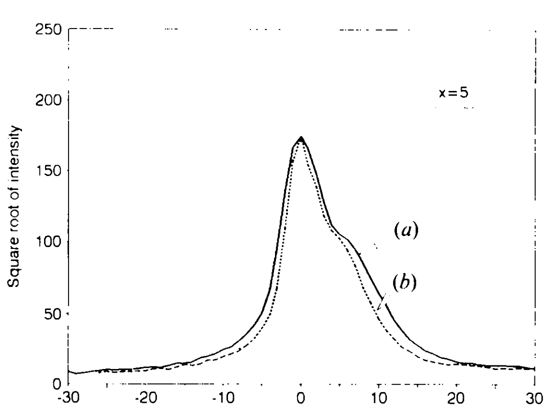

Fig. 4. (004)Si rocking curves (square root of intensity), measured at point $x = 5$ (shown in Fig. 1), (a) without and (b) with ultrasonic excitation.

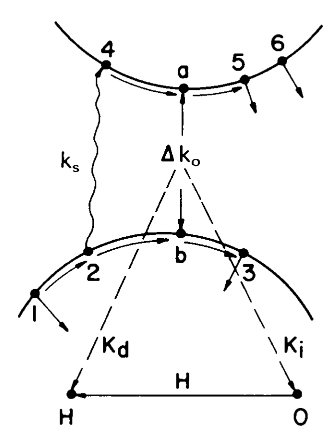

Fig. 5. Dispersion surface for X-rays inside a crystal. K_i and K_d are the wave vectors of the incident and diffracted X-rays, H is the vector of the reciprocal lattice, k_s is the ultrasound wave vector and Δk_o is the band gap in the momentum space.

X-rays from the diffracted beam, leading to a narrowing effect of the rocking curves as was observed in the present experiment (see Figs. 3 and 4).

It should be noted that the explanation of the narrowing effect on the basis of X-ray trajectories can be applied strictly to X-ray diffraction in Laue geometry, where X-ray beams inside the crystal are well defined. Our experimental results were obtained in Bragg geometry, where the introduction of X-ray trajectories meets some difficulties owing to the imaginary parts of the X-ray wave vectors. However, it has been demonstrated in a series of papers [see, for example, Bonse (1964) and Gronkowski & Malgrange (1984)] that the concept of X-ray trajectories can be used even in the Bragg case, at least outside the total-reflection region. Because the narrowing effect is related mostly to the modification of the tails of rocking curves, it seems that it can be treated in the framework of trajectories.

Note also that modification of X-ray trajectories in the elastically deformed crystals without US was studied in detail [see, for example, Hart & Milne (1971)]. In the case of small strain gradients b,

$$B < 1, \quad B = 2bH/\Delta k_o^2, \tag{4}$$

X-rays propagate through the crystal tuning 'adiabatically' to the distorted atomic planes. In principle, the same result was obtained in crystals deformed by low-frequency ($\lambda_s >> \tau$) US (Zheng, Zarka, Capelle, Detaint & Schwartzel, 1989). Adiabatic movement of X-rays is destroyed at large strain gradients ($B \geq 1$) owing to interbranch scattering processes, having a probability $f_o = \exp(-\pi/2B)$ (Chukhovskii & Petrashen, 1977; Lukas & Kulda, 1989). From the physical point of view, the interbranch scattering plays an essential role when the strain value δ on the reduced extinction length, $\tau/2\pi$, exceeds the angular half-width of the diffraction maximum, $\Delta\Theta_o/2 = \Delta k_o/2H$:

$$\delta = b\tau/2\pi \geq \Delta k_o/2H. \tag{5}$$

The condition $B \geq 1$ follows immediately from (5), using the B definition [see (4)]. High-frequency US creates a new direct channel of interbranch scattering as shown in Fig. 5. Since the probability of this process is $f_1 = 1 - \exp[-\pi(Hw)^2/(2B)]$ (Iolin, 1987; Iolin, Raitman, Kuvaldin & Zolotoyabko, 1988), it operates effectively at small strain gradients ($B < 1$) and weak US ($Hw < 1$) if only $(Hw)^2 \simeq B$. This is a result of angular satellites with width $\Delta\Theta_1 = (\Delta k_o/H)Hw$ [see (3)], which create a new extinction length $\tau_1 = \tau/Hw$. Correspondingly, condition (5) should be rewritten in the form

$$\delta = b\tau_1/2\pi \geq \Delta\Theta_1/2. \tag{6}$$

From (6), it follows that the significant role of US-induced interbranch scattering is at $(Hw)^2 \simeq B$.

Thus, high-frequency US drastically modifies X-ray propagation inside the strained crystal at small strain gradients $B < 1$, leading to some new effects, such as the narrowing effect of double-crystal X-ray diffraction rocking curves presented here. Since the probability of the interbranch jump, which is responsible for the modification of X-ray trajectories, depends exponentially on the strain gradient, the narrowing effect should be very sensitive to the lattice strain. In order to emphasize the strain sensitivity, the rocking curves with US were subtracted from those without US. For example, the resultant curve obtained by this method at point $x = 2$ (see Fig. 6) exhibits asymmetry that was difficult to resolve in the original rocking curve (see Fig. 3). This asymmetry is a precursor of the shoulder formation, which was clearly observed in the original rocking curves only at points $x = 5$ and $x = 6$ (Figs. 2 and 4), points that are related to a stronger distorted region in the sample. The angular position of the right-hand peak in Fig. 6 and, consequently, the position of the

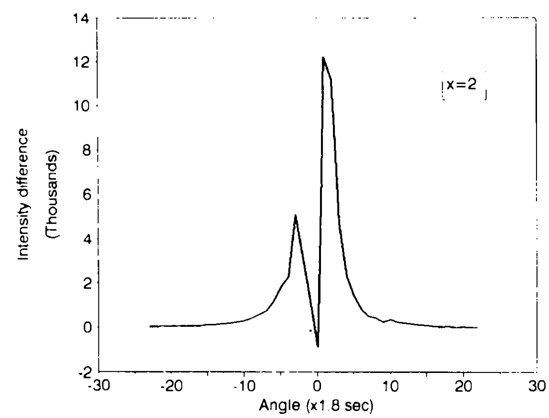

Fig. 6. Resultant curve obtained at point $x = 2$ by subtraction of the rocking measured with ultrasound from the one without ultrasonic excitation (shown in Fig. 3).

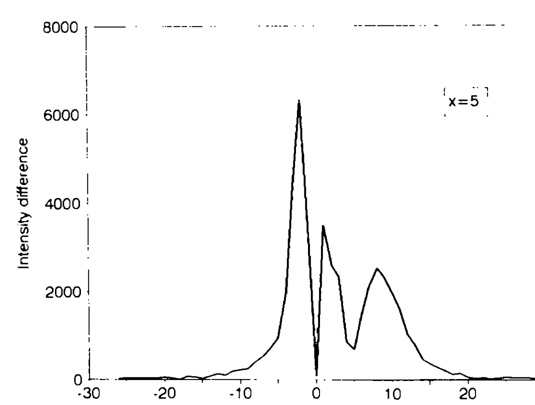

Fig. 7. Resultant curve obtained at point $x = 5$ by subtraction of the rocking curve measured with ultrasound from the one without ultrasonic excitation (shown in Fig. 4).

shoulder precursor in Fig. 3, corresponds to the strain value $\delta \simeq 2 \times 10^{-5}$ at point $x = 2$, which is almost one order of magnitude lower compared with the strain value extracted from the rocking curve without US at point $x = 6$. Thus, the combined use of X-ray diffraction and high-frequency US allows the earlier detection of strain formation. The resultant curve obtained at $x = 5$ (see Fig. 7) magnifies even more the asymmetry already observed in the original rocking curve (see Fig. 4) by exhibiting an additional peak at the shoulder position. These experimental data give a convincing proof of the narrowing of rocking curves under US excitation in strained crystals and of the enhancement of the strain sensitivity of X-ray diffraction measurements.

4. Concluding remarks

It has been demonstrated that double-crystal X-ray diffraction combined with high-frequency ultrasound is a unique method to study the dispersion surface of X-rays and, consequently, small strains in distorted crystals. Ultrasound-induced transitions between the branches of the dispersion surface in a strained crystal modify the X-ray trajectories and assist in rejection of part of the X-rays from the diffraction process. This modification affects mainly the points of the dispersion surface which were excited originally by the strain gradient. As a result, a narrowing effect of the rocking curves is obtained which is sensitive to small lattice distortions. Measurements with silicon crystals showed a substantial increase of strain sensitivity compared with the conventional X-ray diffraction technique.

This work was supported by the Israel Ministry of Science and Technology and Schlesinger Fund (grant no. 040-515). It was also partly supported by the Henri Gutwirth Fund for the Promotion of Research (no. 040-498). One of the authors (YK) would also like to thank the Fund for the Promotion of Research at Technion.

References

BONSE, U. (1964). *Z. Phys.* **177**, 385–423.

CHAPMAN L. D., COLELLA, R. & BRAY, R. (1983). *Phys. Rev. B*, **27**, 2264–2277.

CHUKHOVSKII, F. & PETRASHEN, P. (1977). *Acta Cryst.* A**33**, 311–319.

ENTIN, I. & ASSUR, K. (1981). *Acta Cryst.* A**34**, 769–774.

GRONKOWSKI, J. & MALGRANGE, C. (1984). *Acta Cryst.* A**40**, 507–514.

HART, M. & MILNE, A. D. (1971). *Acta Cryst.* A**27**, 430–435.

IOLIN, E. (1987). Preprint LAFi-102. Physics Institute of the Latvian Academy of Sciences, Salaspils, Latvia.

IOLIN, E., RAITMAN, E., KUVALDIN, B. & ZOLOTOYABKO, E. (1988). *Sov. Phys. JETP*, **67**, 989–997.

KATO, N. (1963). *J. Phys. Soc. Jpn*, **18**, 1785–1791.

KATO, N. (1964). *J. Phys. Soc. Jpn*, **19**, 67–71, 971–985.

KOHLER, R., MOHLING, W. & PEIBST, H. (1974). *Phys. Status Solidi (B)*, **61**, 173–180.

LUKAS, P. & KULDA, J. (1989). *Phys. Status Solidi B*, **156**, 41–48.

PENNING, P. (1966). *Philips Res. Rep.* **21**, 1–109.

PENNING, P. & POLDER, D. (1961). *Philips Res. Rep.* **16**, 419–440.

ZHENG, Y., ZARKA, A., CAPELLE, B., DETAINT, J. & SCHWARTZEL, J. (1989). *Acta Cryst.* A**45**, 275–285.

ZOLOTOYABKO, E. (1992). *Non-Stoichiometry in Semiconductors*, edited by K. J. BACHMAN, H. L. HWANG & C. SCHWAB, pp. 39–44. Amsterdam: North-Holland.

ZOLOTOYABKO, E., JACOBSOHN, E., SHECHTMAN, D., KANTOR, B. & SALZMAN, J. (1992). *J. Appl. Phys.* **71**, 3134–3137.

ZOLOTOYABKO, E. & PANOV, V. (1992). *Acta Cryst.* A**48**, 225–231.